

Diffuse x-ray scattering from misfit and threading dislocations in PbTe/BaF<sub>2</sub>/Si(111) thin layers

S. Daniš and V. Holý

*Department of Physics of Electronic Structures, Charles University, Ke Karlovu 5, 121 16 Prague, Czech Republic*

(Received 8 October 2005; published 4 January 2006)

Diffuse x-ray scattering from epitaxial PbTe layers on Si(111) is analyzed both theoretically and experimentally. Reciprocal-space maps and x-ray diffraction profiles are measured and simulated for symmetrical and asymmetrical diffractions as well. The intensity distribution of diffusively scattered radiation is simulated within the statistical theory of x-ray scattering. Both types of expected defects—misfit and threading dislocations—are discussed. Comparing simulated maps to measured ones we can distinguish between contributions arising from misfit and threading dislocations. In the case of PbTe thin layers, the majority diffuse scattering comes from misfit dislocations.

DOI: [10.1103/PhysRevB.73.014102](https://doi.org/10.1103/PhysRevB.73.014102)

PACS number(s): 61.10.Dp, 61.72.Lk, 68.55.–a

## I. INTRODUCTION

X-ray scattering is widely used for thin film and epitaxial layer characterization. Usually, only one experimental parameter is used for the structure characterization—full width at half maximum (FWHM) of a scattered intensity profile. Little attention is paid to the shape of the intensity distribution of diffusely scattered radiation in reciprocal space.

Several papers have dealt with the analysis of the reciprocal-space distribution of the intensity diffracted from thin layers with dislocations. Ayers<sup>1</sup> elaborated a model which is frequently applied to threading dislocation density determination in various types of semiconductor heterostructures. Threading dislocations cause a decrease of mobility of charge carriers, i.e., they affect transport properties of the system. His model is based on the measurement of FWHM of different diffractions and then plotting FWHM (Ref. 2) against  $\tan^2 \theta$ , where  $\theta$  is the Bragg angle. Threading dislocation density can be determined either using the slope of linear dependence FWHM— $\tan^2 \theta$  or from the intercept with the ordinate. Nevertheless, only for the FWHM we cannot determine the type of defects. In contrast to FWHM, reciprocal-space maps, i.e., intensity distribution of scattered radiation around reciprocal lattice point, can be used for the determination of the type and concentration of the defects.

Krivoglaz<sup>2</sup> built up a general theoretical description of diffuse scattering connected to the given defect within the layer. This model is routinely used in powder x-ray diffraction. However, using high-resolution x-ray diffraction and reciprocal-space maps (RSM), we are able to analyze the diffusely scattered x rays in more precise way.

Kaganer *et al.*<sup>3</sup> used diffuse scattering from epitaxial layers for the determination of misfit dislocation density in semiconductor heterostructures. He discussed the effect of correlation in dislocation positions and density inhomogeneities on diffraction profile as well. Daniš *et al.*<sup>4</sup> studied diffuse scattering from threading dislocation in epitaxial GaN layers. Correlation in dislocation positions were treated in different ways by using Kubo expansion formulas.

However, Kaganer<sup>3</sup> and Daniš<sup>4</sup> dealt only with one type of dislocation—misfit or threading. Actually, misfit and threading dislocations can coexist in the disturbed layer and both of them contribute to diffuse scattering. The analysis of

experimental data is very complicated if several defect types are present in the investigated sample. This situation is very common—due to a mismatch of layer and substrate lattice parameters we may expect creation of misfit dislocations at the interface. Misfit dislocations can generate threading dislocation segments. Both these types of defect affect the shape, i.e., FWHM, of the intensity profile.

In this paper, we present a method of how to distinguish the contributions of threading and misfit dislocations to the RSM. The method is based on the Krivoglaz<sup>2</sup> theory.

The paper is organized as follows: in Sec. II we introduce basic formalism from the kinematical approximation needed for the description of diffuse scattering. In Sec. III experimental conditions as well as experimental results will be presented. Section IV is devoted to discussion and in Sec. IV conclusions are presented.

## II. INTENSITY OF DIFFUSE X-RAY SCATTERING

Our aim is to calculate the intensity of diffusely scattered x rays from an epitaxial layer of PbTe containing both misfit and threading dislocations. At first, we introduce essential formalism used in our work. In the second part of this section we focus on a particular case of defects in a epitaxial PbTe layer.

## A. Diffuse scattering within the kinematical approximation

In an experiment, we usually measure intensity distribution  $I(\mathbf{Q})$  of scattered x rays around a reciprocal lattice point (RLP) given by a wave vector  $\mathbf{Q}$ . It is convenient to introduce the wave-vector deviation  $\mathbf{q} = \mathbf{Q} - \mathbf{Q}_0$  from the nearest RLP vector  $\mathbf{Q}_0$ . For the reader's convenience we summarize the necessary theory according to Kaganer's work.<sup>3</sup>

In the kinematical approximation, the intensity of diffuse scattering by a layer of thickness  $T$  ( $-T < z < 0$ ) is given as a Fourier integral

$$I(\mathbf{q}) = A_{\mathbf{Q}} \int_{z \in (-T, 0)} d^3 \mathbf{r} \int_{z' \in (-T, 0)} d^3 \mathbf{r}' e^{-i(\mathbf{q} \cdot \mathbf{r} - \mathbf{q}^* \cdot \mathbf{r}')} G(\mathbf{r} - \mathbf{r}'), \quad (1)$$

where  $A_{\mathbf{Q}}$  is a constant containing a square of the sample polarizability, among others, and  $G(\mathbf{r} - \mathbf{r}')$  is the correlation

function of the deformation field caused by the defects

$$G(\mathbf{r}, \mathbf{r}') = \langle \exp\{-i\mathbf{Q} \cdot [\mathbf{u}(\mathbf{r}) - \mathbf{u}(\mathbf{r}')]\} \rangle. \quad (2)$$

$\mathbf{u}(\mathbf{r})$  denotes the random shift of the atom in position  $\mathbf{r}$  due to the defects and  $\mathbf{Q}$  is the diffraction vector. The averaging  $\langle \rangle$  is performed over the ensemble of all defect configurations.

If we assume that the system is laterally uniform, the integral (1) can be simplified to the form (assuming a coplanar geometry)

$$I(q_x, q_z) = A_{\mathbf{Q}} \int_{-\infty}^{\infty} dx \int_{-T}^0 dz \int_{-T}^0 dz' e^{-i[q_x x + q_z(z-z')]} \times e^{\mu(z+z')} G(x, z, z'), \quad (3)$$

where  $\mu$  is the linear absorption coefficient. Integration over the  $y$  coordinate was performed in an evaluation of (3) (i.e., a wide open detector is used during experiment).

An explicit formula for the correlation function  $G(x, z, z')$  was derived by Krivoglaz,<sup>2</sup> who rewrote  $G(x, z, z')$  into the exponential form

$$G(x, z, z') = \exp\{-T(x, z, z')\}, \quad (4)$$

where  $T(x, z, z')$  is also called the correlation function. In the case of uncorrelated misfit dislocations parallel to the  $y$  axis, the correlation function  $T(x, z, z')$  has the following form:

$$T(x, z, z') = \sum_{\alpha} \varrho_{\alpha} \int_{-\infty}^{\infty} dx' \{1 - e^{i\mathbf{Q} \cdot [\mathbf{u}_{\alpha}(x', z) - \mathbf{u}_{\alpha}(x' - x, z')]} \}, \quad (5)$$

and for threading dislocations we obtain

$$T(x, z, z') = \sum_{\alpha} \varrho_{\alpha} \int d^2 \mathbf{r}'' \{1 - e^{i\mathbf{Q} \cdot [\mathbf{u}_{\alpha}(\mathbf{r} - \mathbf{r}'', z) - \mathbf{u}_{\alpha}(\mathbf{r}' - \mathbf{r}'', z')]} \}, \quad (6)$$

where in both equations we sum over all types of the defects. If the dislocation density is large enough, one can apply the Taylor expansion to the dot product  $\mathbf{Q} \cdot [\mathbf{u}(\mathbf{r} - \mathbf{r}'', z) - \mathbf{u}(\mathbf{r}' - \mathbf{r}'', z')]$ , yielding

$$\mathbf{Q} \cdot [\mathbf{u}(\mathbf{r} - \mathbf{r}'', z) - \mathbf{u}(\mathbf{r}' - \mathbf{r}'', z')] = \mathbf{R} \cdot \nabla[\mathbf{Q} \cdot \mathbf{u}(\mathbf{r}'', z)], \quad (7)$$

where the vector  $\mathbf{R} = (\mathbf{r} - \mathbf{r}', z - z') = (x, 0, z - z')$ . Actually, because we are doing integration over  $y$  in (3), the  $x$  in  $\mathbf{R}$  is equal to  $|\mathbf{r} - \mathbf{r}'|$ .

In the case of threading dislocations, by substituting from Eq. (7) into (6) and using the expansion  $\exp(ix) = 1 + ix - \frac{1}{2}x^2$ , we obtain the following formula for the correlation function:

$$T(x, z, z') = \sum_{\alpha} \varrho_{\alpha} \int d^2 \mathbf{r}'' \left\{ i \left( x \frac{\partial \mathbf{Q} \cdot \mathbf{u}(\mathbf{r}'', z)}{\partial x} + (z - z') \frac{\partial \mathbf{Q} \cdot \mathbf{u}(\mathbf{r}'', z)}{\partial z} \right) + \frac{1}{2} \left( x \frac{\partial \mathbf{Q} \cdot \mathbf{u}(\mathbf{r}'', z)}{\partial x} + (z - z') \frac{\partial \mathbf{Q} \cdot \mathbf{u}(\mathbf{r}'', z)}{\partial z} \right)^2 \right\}. \quad (8)$$

The imaginary part of  $T(x, z, z')$  is responsible for a shift of

the intensity maximum in the  $(q_x, q_z)$  plane. This shift is caused by an average strain induced in the layer by the defects. The real part of the correlation function describes the shape of the intensity profile of the scattered radiation.

It can be easily shown<sup>3</sup> that, within this so-called *high-density approximation*, the real part of the correlation function  $T(x, z, z')$  is a quadratic form both in  $x$  and  $(z - z')$ . This implies a Gaussian profile of the scattered intensity along the  $q_x$  direction. Kaganer<sup>3</sup> proved that for misfit dislocations this approximation is valid if  $L \ll T$ , where  $L$  is the mean distance between misfit dislocations and  $T$  is the layer thickness. However, such simple condition can not be stated for threading dislocations. In this case we have to check the shape of intensity distribution along the  $q_x$  direction—if it is Gaussian, we can use the high-density approximation.

The approximation described above significantly simplifies the calculation of the intensity distribution  $I(q_x, q_z)$  near a RLP, see Eq. (3). As mentioned above, the shape of the intensity distribution  $I(q_x, q_z)$  is fully determined by the *real* part of the correlation function (8). Substituting the real part of (8) into Eq. (3), we get

$$I(q_x, q_z) = A_{\mathbf{h}} \int_{-\infty}^{\infty} dx \int_{-T}^0 dz \int_{-T}^0 dz' e^{-i[q_x x + q_z(z-z')]} e^{\mu(z+z')} \times e^{-A(z)x^2 - B(z)x(z-z') - C(z)(z-z')^2}, \quad (9)$$

where

$$A(z) = \frac{1}{2} \int d^2 \mathbf{r}'' \left( \frac{\partial \mathbf{Q} \cdot \mathbf{u}(\mathbf{r}'', z)}{\partial x} \right)^2 \quad (10)$$

$$B(z) = \frac{1}{2} \int d^2 \mathbf{r}'' \frac{\partial \mathbf{Q} \cdot \mathbf{u}(\mathbf{r}'', z)}{\partial x} \frac{\partial \mathbf{Q} \cdot \mathbf{u}(\mathbf{r}'', z)}{\partial z} \quad (11)$$

$$C(z) = \frac{1}{2} \int d^2 \mathbf{r}'' \left( \frac{\partial \mathbf{Q} \cdot \mathbf{u}(\mathbf{r}'', z)}{\partial z} \right)^2. \quad (12)$$

For the symmetrical diffraction, i.e., for  $\mathbf{Q}_0 = (0, 0, Q_z)$  and  $B(z) \equiv 0$ , we can easily perform the integration over  $x$ ,

$$I(q_x, q_z) = A_{\mathbf{h}} \int_{-T}^0 dz \int_{-T}^0 dz' \frac{\sqrt{\pi}}{\sqrt{A(z)}} e^{-q_x^2/4A(z)} e^{-iq_z(z-z')} \times e^{\mu(z+z')} e^{-C(z)(z-z')^2}, \quad (13)$$

where integration over  $z$  and  $z'$  have to be evaluated numerically. We can immediately see, that along the  $q_x$  direction the peak shape is Gaussian. For asymmetrical diffraction, i.e.,  $\mathbf{Q} = (Q_x, 0, Q_z)$  and  $B(z) \neq 0$ , the separate integration over  $x$  can be performed as well, however, resulting in a little bit of a complicated formula. For misfit dislocation, we can derive similar relations, indeed.

## B. Misfit and threading dislocations in epitaxial PbTe layers

PbTe crystallizes within the cubic NaCl structure. The main dislocation system is  $\langle 110 \rangle \{100\}$ . Due to a large mismatch between lattice parameters of silicon (substrate,  $a = 5.431 \text{ \AA}$ ) and PbTe ( $a = 6.462 \text{ \AA}$ ), a high density of misfit



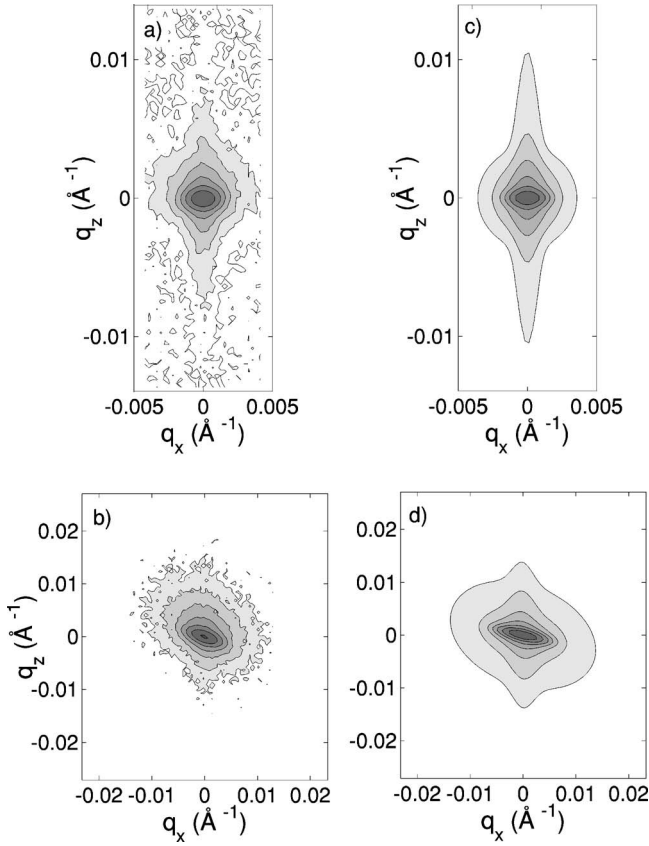


FIG. 3. (a) and (b) show measured reciprocal space maps for symmetrical diffraction 111 (up) and asymmetrical 224 (bottom) of the 1.3  $\mu\text{m}$  thick PbTe layer. (c) and (d) show simulated maps for the same diffractions.

Reciprocal-space maps near several reciprocal lattice points were measured using a laboratory high-resolution x-ray diffractometer. The primary x-ray beam (Cu anode, 40 kV/35 mA) was monochromatized by a four-bounce asymmetrical Ge220 Bartels monochromator; an x-ray mirror was placed in front of the monochromator. The size of the beam irradiating the sample was set to  $0.5 \times 0.5 \text{ mm}^2$  using cross slits. The scattered radiation was analyzed by a three-bounce crystal symmetrical Ge220 channel-cut analyzer and registered with a gas-filled proportional detector.

Figure 3 shows measured diffusely scattered intensity near reciprocal lattice points—111 (symmetrical) and 224 (asymmetrical). As was shown above, the shape of asymmetrical reciprocal-space maps can determine if the diffuse scattering is due to misfit or threading dislocations. As we can see, the shape of measured asymmetrical space is similar to the shape of simulated *misfit* dislocations.

The misfit dislocation density was determined from fitting the measured  $q_x$  scans to the theory above; the results are plotted in Fig. 4. From the fits we have determined the misfit dislocation density is  $\varrho = 1.6 \times 10^4 \text{ cm}^{-1}$ . As is shown in Fig. 4 the intensity profile cannot be explained only by misfit dislocations, especially concerning the tails of the profile. Including diffuse scattering from threading dislocations does not help. Adding the contribution threading dislocations in the correlation function  $T(x, z, z')$  only changes parameters

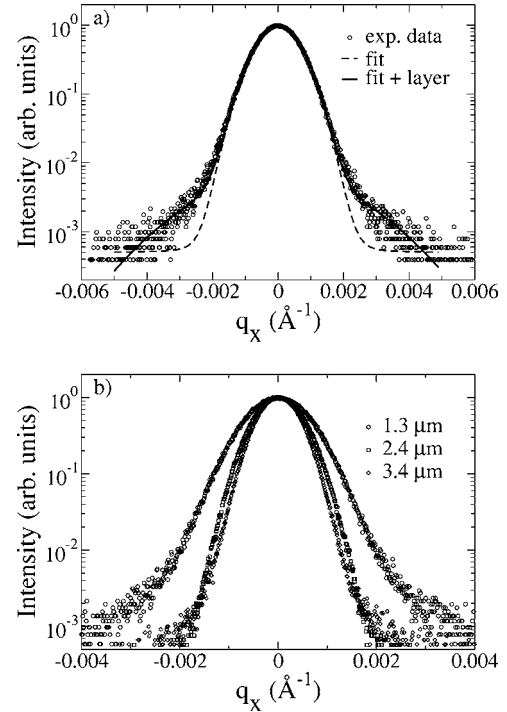


FIG. 4. (a):  $q_x$  scan of the 1.3  $\mu\text{m}$  thick PbTe layer for symmetrical diffraction 111. Points note measured data and the dashed line marks theoretical calculation using the high-density approximation (Gaussian profile with constant background). The solid line denotes sum of the fitted curve (dashed) and the contribution of the disturbed surface layer. See the text for details. (b):  $q_x$  scans for three thickness of the PbTe layer. With increasing thickness of the layer the diffraction profile become narrower.

of the resulting Gaussian profile—the tails remain the same. Even as we did not use the high-density approximation for threading dislocations, we are not able to fit the tails of the diffraction profiles. Finally, we introduced a thin disturbed layer at the top of the PbTe layer which contribute to the diffuse scattering, e.g., due to surface roughness. Since we do not exactly know the type of the defects in this disturbed layer, and even the thickness of it, we define the correlation function  $T(x, z, z')$  of this layer in a general quadratic form  $T(x, z, z') = A_L x^2 + B_L x(z - z') + C_L (z - z')^2$ . This form of correlation function is used in a phenomenological mosaic-block model where the quadratic form is a result of a product of the mosaic-block shape function and deformation within the block.<sup>8</sup> Finally, if we assume that the disturbed layer can be assumed as a small perturbation, then measured intensity is a sum of diffuse scattering originating from misfit dislocations and the intensity of the disturbed layer,  $I = I_{\text{misfit}} + I_{\text{dist. layer}}$ , see Fig. 4.

From the comparison of measured RSMs and simulations using the misfit-dislocation model we determined the density of misfit dislocations to  $1.6 \pm 0.1 \times 10^4 \text{ cm}^{-1}$ . However, this value of the misfit dislocation density is about 3 orders less than the expected misfit dislocation density of a *full relaxed layer* ( $\varrho_{\text{relax}} \sim 10^7 \text{ cm}^{-1}$ ). We have checked the degree of relaxation by measuring reciprocal-space maps over a large area in order to measure asymmetrical diffraction from PbTe

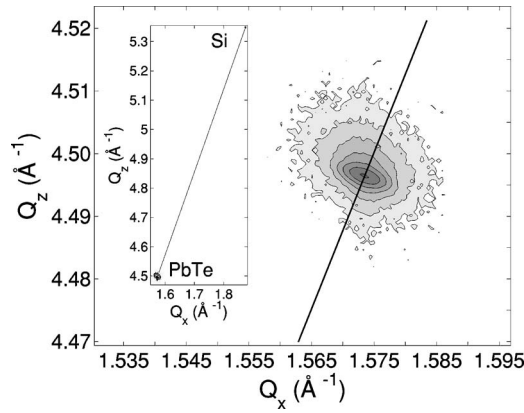


FIG. 5. Reciprocal space maps around RLP 224 of Si (substrate) and PbTe (layer). The layer is fully relaxed.

and Si simultaneously. The result is shown in Fig. 5—the PbTe layer is fully relaxed.

In our theoretical description we did not consider any correlation in dislocation positions. As was shown by Kaganer *et al.*,<sup>3</sup> if a spatial correlation of the dislocation positions takes place, the diffraction profile becomes narrower. Therefore, most likely we observe an *effective* dislocation density  $\gamma\rho$ , where  $\gamma$  is correlation parameter  $\gamma \leq 1$  ( $\gamma=1$  for uncorrelated case). In our case  $\gamma \sim 0.001$ , it implies that misfit dislocations are strongly correlated in their positions. Kaganer<sup>3</sup> reported  $\gamma=0.03$  for the AlSb layer grown on GaAs (misfit 7.9%—compare with 19% for PbTe and Si).

We have determined the misfit dislocation density of PbTe layers with thicknesses 1.3, 2.4, and 3.4  $\mu\text{m}$  grown on the same piece of the substrate. Despite decreasing the FWHM of the intensity profile the dislocation density remains nearly the same, see Table I.

#### IV. DISCUSSION

Statistical kinematical approximation of x-ray scattering was used to describe the diffuse scattering from epitaxial PbTe layers. Two types of defects were considered—misfit and threading dislocations. Threading dislocations were assumed to be of inclined screw origins.

Simulated reciprocal-space maps of misfit dislocations agree quite well to measured data. Diffraction profiles became narrower whereas the dislocation density remains the same. Our results indicate strong correlation in misfit dislocation positions, as well. Contribution of threading dislocations can be neglected. This is shown in Fig. 6 where contri-

TABLE I. Misfit dislocation densities for PbTe layers with different thicknesses. Within the errors, the dislocation density remains the same.

$t$ ( $\mu\text{m}$ )	$\rho$ ( $10^4 \text{ cm}^{-1}$ )
1.3	$1.6 \pm 0.1$
2.4	$1.6 \pm 0.1$
3.4	$1.5 \pm 0.1$

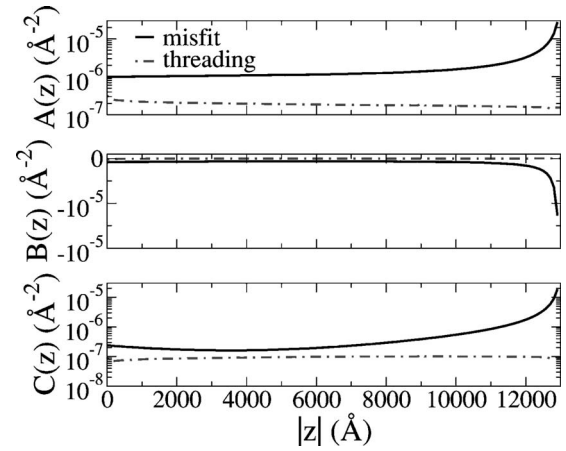


FIG. 6. Coefficients of the quadratic form of correlation function  $T(x, z, z')$  [see Eqs. (10)–(12)] are plotted as a function of the  $z$  coordinate for the  $T=1.3 \mu\text{m}$  thick layer.  $z=0$  means the surface of the layer;  $z=-T$  denotes the layer-substrate interface. Following dislocation densities were chosen:  $\rho_m=1.6 \times 10^{-4} \text{ cm}^{-1}$ ;  $\rho_{th}=10^8 \text{ cm}^{-2}$ . The coefficients of misfit dislocation are larger (in absolute value) than the ones for threading dislocation. Thus, the main contribution to diffuse scattering comes from misfit dislocations.

butions to quadratic-form coefficients of  $T(x, z, z')$  are plotted in the case of asymmetrical diffraction 224.

To our knowledge, any detailed analysis of x-ray diffuse scattering from PbTe layers was not published, so far. Several authors<sup>9,10</sup> dealt only with the FWHM of the diffraction profile. These authors supposed that the diffuse scattering is mainly due to threading dislocations. Only simple analysis based on Ayers<sup>1</sup> approach has been performed. Threading dislocation density was reported to be of order of  $\rho_{th} \sim 10^8 \text{ cm}^{-2}$ . The thickness dependence of  $\rho_{th}$  was found to follow the exponential law  $\rho_{th} \sim T^{-\alpha}$ , however some different values of  $\alpha$  have been reported. While a  $T^{-1}$  law follows easily from probability considerations,<sup>11</sup> deviations from this inverse power law still await a convincing explanation.

However, if there are several types of dislocations (and/or other defects) present within the layer, we have to analyze the diffuse scattering more carefully. Sometimes reciprocal-space maps can be helpful in order to uncover the main source of diffuse scattering. This implies that without thorough investigation of reciprocal-space maps, the only application of FWHM can be inaccurate.

#### V. CONCLUSION

Diffuse scattering from thin epitaxial layer of PbTe grown on Si(111) substrates was examined. It was shown that the intensity distribution of diffusely scattered radiation is mainly caused by misfit dislocations. The contribution of threading dislocations (inclined screw dislocations) is negligible. The misfit dislocation density remains the same (within the errors) for several layer thicknesses.

#### ACKNOWLEDGMENTS

This work was supported by the Ministry of Education of the Czech Republic, Program No. MSM 0021620834. Partial

financial support by the Grant Agency of Czech Republic (Project No. 202/04/P258) is gratefully appreciated. The authors would like to thank Hans Zogg (Thin Film Physics

Group, Swiss Federal Institute of Technology, ETH-Teil Technopark, CH-8005 Zürich, Switzerland) for providing samples.

- 
- <sup>1</sup>J. E. Ayers, *J. Cryst. Growth* **135**, 71 (1994).  
<sup>2</sup>M. A. Krivoglaz, *X-Ray and Neutron Diffraction in Nonideal Crystals* (Springer, Berlin 1996); R. Barabash, *Mater. Sci. Eng., A* **A309–310**, 49 (2001).  
<sup>3</sup>V. M. Kaganer, R. Kohler, M. Schmidbauer, R. Opitz, and B. Jenichen, *Phys. Rev. B* **55**, 1793 (1997).  
<sup>4</sup>S. Daniš, V. Holý, Z. Zhong, G. Bauer, and O. Ambacher, *Appl. Phys. Lett.* **85**(15), 3065 (2004).  
<sup>5</sup>G. Springholz, A. Y. Ueta, N. Frank, and G. Bauer, *Appl. Phys. Lett.* **69**, 2822 (1996).  
<sup>6</sup>S. J. Shaibani and P. M. Hazzledine, *Philos. Mag. A* **44**, 657 (1981).  
<sup>7</sup>H. Zogg, S. Blunier, A. Fach, C. Maissen, P. Müller, S. Teodoropol, V. Meyer, G. Kostorz, A. Dommann, and T. Richmond, *Phys. Rev. B* **50**, 10801 (1994).  
<sup>8</sup>V. Holý, J. Kuběna, E. Abramof, K. Lischka, A. Pesek, and E. Koppensteiner, *J. Appl. Phys.* **74**, 1736 (1993).  
<sup>9</sup>D. Zimin, Ph.D thesis, ETH Zurich.  
<sup>10</sup>P. Müller, H. Zogg, A. Fach, J. John, C. Paglino, A. N. Tiwari, M. Krejci, and G. Kostorz, *Phys. Rev. Lett.* **78**, 3007 (1997).  
<sup>11</sup>H. Kroemer, T. Y. Liu, and P. M. Petroff, *J. Cryst. Growth* **95**, 96 (1989).